SANDIA REPORT
SAND2018-13174
Printed November 2018

Sandia National Laboratories

Acoustic Chamber Characterization

Edward O'Brien, Timothy Kypta, Joshua Stanford, Hy Tran

Prepared by
Sandia National Laboratories
Albuquerque, New Mexico
87185 and Livermore,
California 94550

Issued by Sandia National Laboratories, operated for the United States Department of Energy by National Technology & Engineering Solutions of Sandia, LLC.

Available to DOE and DOE contractors from
U.S. Department of Energy
Office of Scientific and Technical Information
P.O. Box 62
Oak Ridge, TN 37831

Telephone: (865) 576-8401
Facsimile: (865) 576-5728
E-Mail: reports@osti.gov
Online ordering: http://www.osti.gov/scitech

Available to the public from
U.S. Department of Commerce
National Technical Information Service
5301 Shawnee Rd
Alexandria, VA 22312

Telephone: (800) 553-6847
Facsimile: (703) 605-6900
E-Mail: orders@ntis.gov
Online order: https://classic.ntis.gov/help/order-methods/

ABSTRACT

The basis of this project was to characterize the various uncertainty contributors of an acoustic chamber. The acoustic chamber will be used to calibrate and characterize infrasound sensors used in the field in the frequency range of 0.001 Hz to 4 Hz. The components characterized include the internal volume of the chamber, the piston area of the speaker creating the dynamic sound wave, the environmental stabilization of the chamber and the chamber's leak rate. Also, the resonant frequency of the chamber was evaluated and found to be far outside the frequency band of interest.

ACKNOWLEDGEMENTS

The authors would like to acknowledge Randy Rembold and John Merchant for supporting and funding this project through the Defense Threat Reduction Agency (DTRA). We would also like to thank Henry Lorenzo and Monico Lucero of Manufacturing Liaison working along with Robert Jones and Tony Bryce of Mechanical Calibration for performing the dimensional measurements of the Acoustic Chamber. We would like to thank Curt Mowry and Adam Pimentel of Organization 01852 for measuring the density of a sample of the fiber-reinforced material of the grate. We would also like to thank the two main reviewers of this document Raegan Johnson and Dalaila Mora whose comments/suggestions helped improve and clarify this report.

CONTENTS

LIST OF FIGURES

LIST OF TABLES

This page left blank

ACRONYMS AND DEFINITIONS

Abbreviation	Definition
SNL	Sandia National Laboratories
FACT	Facility for Acceptance, Calibration and Testing
PSL	Primary Standards Laboratory
MPE	maximum permissible error
CMM	coordinate measuring machine

1. INTRODUCTION

This report summarizes the results of a characterization study on an acoustic chamber located at the Sandia National Laboratories (SNL) Facility for Acceptance, Calibration and Testing (FACT) site. The study was performed in an effort to support calibration and characterization of infrasound sensors. The acoustic chamber was designed and constructed by the National Center for Physical Acoustics (NCPA) at the University of Mississippi for SNL [1]. The project goal was to evaluate and characterize the contributing measurement uncertainties of the acoustic chamber when performing calibrations of infrasound sensors. This acoustic chamber will be used to characterize and calibrate infrasound sensors in the frequency range of 0.001 Hz to 4 Hz.

Many different contributions need to be considered when determining the appropriate measurement uncertainty analysis. The primary contributors that were studied include the interior volume of the chamber, the internal temperature and the pressure in the acoustic chamber. These parameters, along with their associated uncertainties, should be applied to a measurement equation. The sensitivity coefficients of each of these contributors should be determined and subsequently applied to the measurement equation when calculating the total measurement uncertainty. The resonant frequency of the chamber was also evaluated to ensure that the resonance is outside the frequency range of interest. A static leak test was performed to ensure that the acoustic chamber was capable of remaining at a constant pressure.

Some parameters that were not included in this study are the chamber stiffness, calibration and uncertainties of measurement standards as well as repeatability and reproducibility of infrasonic measurements. In regard to the chamber stiffness, the walls of the acoustic chamber flex in response to pressure differentials and this modifies the pressure inside of the chamber. However, since the chamber is cylindrical and has one-inch thick walls of metal, it was assumed that this flexing would be insignificant. Cylindrical acoustic chambers are much stiffer than rectangular acoustic chambers [2]. The uniformity of the field space of the acoustic chamber was not evaluated but should be uniform throughout the cavity for the frequency band of interest [3]. This is an additional parameter that could be evaluated in the future.

In regard to the measurement standards, the standards that will be used for the calibrations were not evaluated as part of the acoustic chamber characterization and uncertainty analysis because we only focused on the contributors related to the acoustic chamber itself. However, it is extremely important to include the uncertainties related to the measurement standards in the final uncertainty budget. The uncertainty of the measurement standards along with the repeatability of the measurements are vital contributors that must be included in the final uncertainty analysis but are not discussed in this report since this is an evaluation of the acoustic chamber and not the measurement process.

2. DETERMINING THE INTERNAL VOLUME OF THE ACOUSTIC CHAMBER

As mentioned earlier, the internal volume of the acoustic chamber is an important contributor to the uncertainty of the measurement for the calibration of infrasound sensors. The internal volume of the acoustic chamber was determined and will be reported as a rectangular distribution. Many acoustic systems use a pistonphone as the sound source. This sound source uses a closed coupling volume to generate a precise sound pressure. This is based upon the mechanical piston that is driven at a specific rate, pushing a fixed volume of air to the infrasound sensors [4]. In the experiment described here, a modified speaker will be used to perform these measurements. The displacement of the speaker was evaluated and is discussed later in the report.

The following pieces of equipment were used for measuring the dimensions of the FACT chamber:

- Faro Laser tracker, Primary Standards Laboratory (PSL) asset # SNL-9408; maximum permissible error (MPE) 0.016 mm + 1 μm/m (radial distance); 0.02 mm + 5 μm/m (transverse distance)
- Faro Edge arm with scanner, PSL asset # SNL-9757; volumetric MPE (using point probe) is 0.041 mm over the workspace; the scanner is not certified
- Zeiss Contura Coordinate Measuring Machine (CMM), PSL asset # SNL-7399; MPE 0.0023 mm + 3.3 5 μm/m; this was used to check the performance of the Faro arm optical scanner. Preliminary data comparing SNL-9757 with the scanner to SNL-7399 show agreement to ± 0.013 mm. This can be treated as a rectangular distribution.

As described above, a cylindrical or spherical chamber is much stiffer than a rectangular or square chamber, and as such, will reduce the volume contribution in the uncertainty. Unfortunately, the volume in a cylindrical chamber is much more difficult to quantify due to its curved surfaces. For the evaluation of the volume of the acoustic chamber, the chamber was split into three separate sections: the door hemisphere, the far end hemisphere and the cylinder body, shown below in Figure 1.

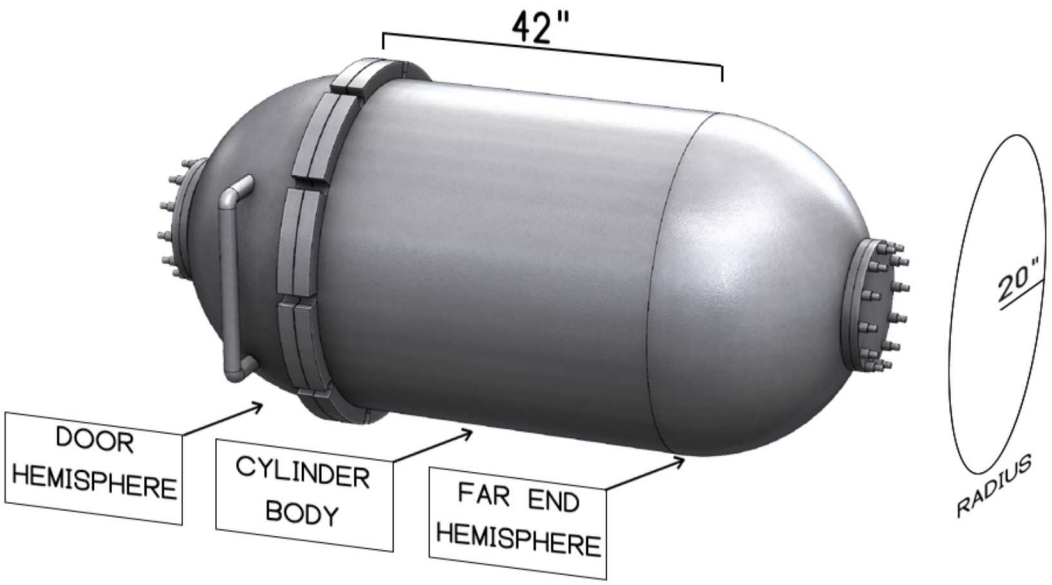

Figure 1: Acoustic Chamber

The contributors for the dimensional measurements include the uncertainty of the measurement equipment, which was < ± 0.013 mm for individual points or related geometry features. As well as the uncertainty associated with the geometry imperfections internal to the acoustic chamber, which is typically in the order of mm. These measurement uncertainties are both Type B contributors, which means that the evaluation of this uncertainty is by means other than a statistical analysis [5]. The geometry imperfections in the acoustic chamber dominate the uncertainty estimate. The maximum diameter (radius) and minimum diameter of the internal dimensions of the acoustic chamber were used as the bounds for the rectangular distribution. The reference temperature for dimensional (and resulting volumetric) measurements is 20 °C and the measurements were made at ambient temperature which was 2 °C. The resulting impact of the temperature difference is not significant relative to the overall stated uncertainty for the volumetric measurements.

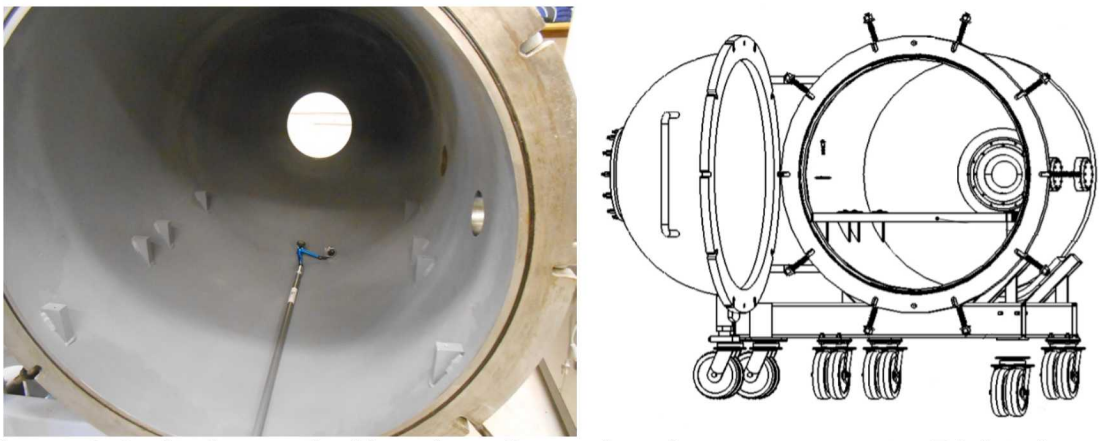

Figure 2: Left: Acoustic Chamber dimensional measurements. Right: Acoustic Chamber drawing [6]

2.1. The Door Hemisphere

This section describes the geometry calculations and its associated uncertainty contribution to the measurement for the volume of the door hemisphere. The door hemisphere was modeled as a short cylindrical section, followed by a truncated hemisphere, sketched as shown in Figure 3.

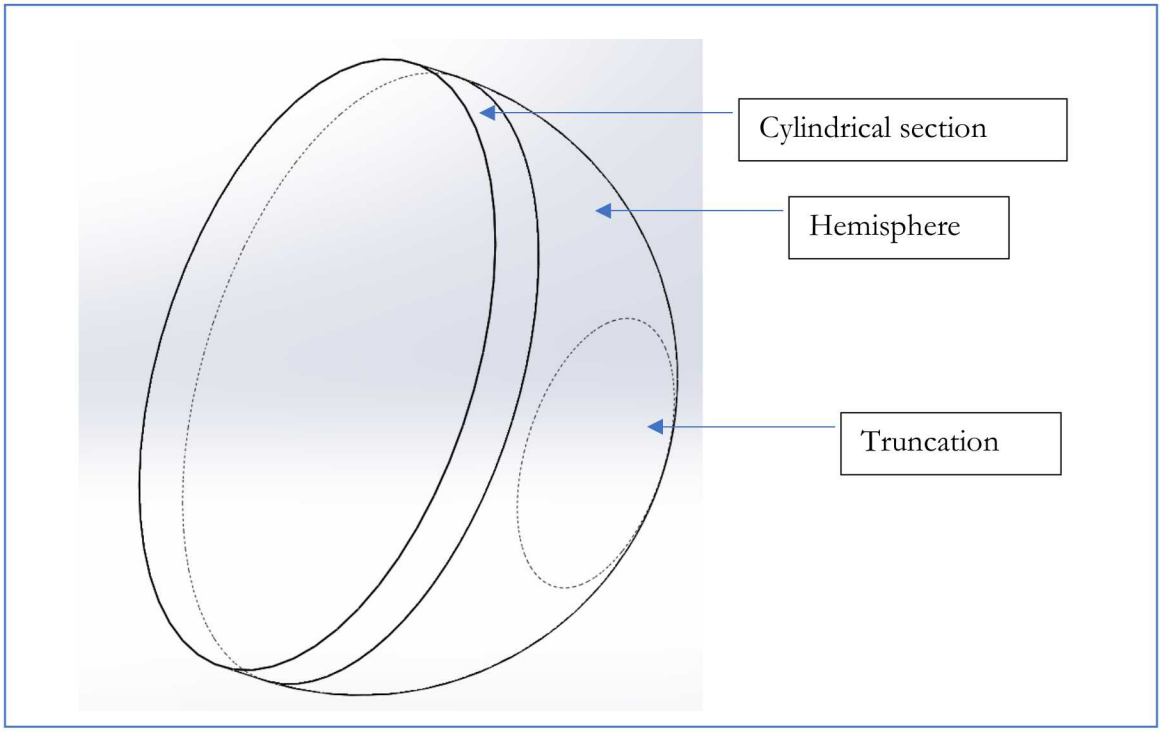

Figure 3. Sketch of model for door hemisphere

The door hemisphere was measured using an articulating arm CMM, the Faro laser tracker, and was modeled as a pure sphere. A cartesian system was set up with the direction of the "x" axis going into the sphere (positive direction from the large opening towards the truncation); the origin was determined using the closing flange as x=0, and y=z=0 at the center of the sphere. Neither the

cylindrical section nor the truncation was measured; it was assumed that the shape of the door was a cylindrical hemisphere. The truncation at the far end was not measured, instead, the dimension of the truncation was assumed using symmetry.

The length of the cylindrical section was measured to be 46.76 mm. The measured diameter of the cylindrical section ranges from 1015.6 mm to 1022.6 mm; this is also the diameter of the hemisphere.

The truncation measurement has much simpler surfaces to measure since it is flat—the diameter is 324.215 mm, and the reported minimum and maximum is 0.280 mm (in ASME GD&T, this is a total deviation, so it is interpreted as ± 0.14 mm). Therefore, the truncation ranges from 324.075 mm to 324.355 mm for the diameter.

Next, the volume of the spherical cap was calculated and then subtracted from the volume of the hemisphere. The minimum cap volume occurs when the hemisphere diameter and cap diameter are minimized while the maximum volume occurs when the cap diameter and hemisphere diameter are maximized. The volume of the door was calculated using the formula for the volume of a spherical cap [7]. Given the geometry shown in Figure 4, the volume of the cap is:

$$V = (\frac{1}{6})\pi h(3a^2 + h^2)$$

From trigonometry:

$$R^2 = (R - h)^2 + a^2$$

$$h = R - \sqrt{R^2 - a^2}$$

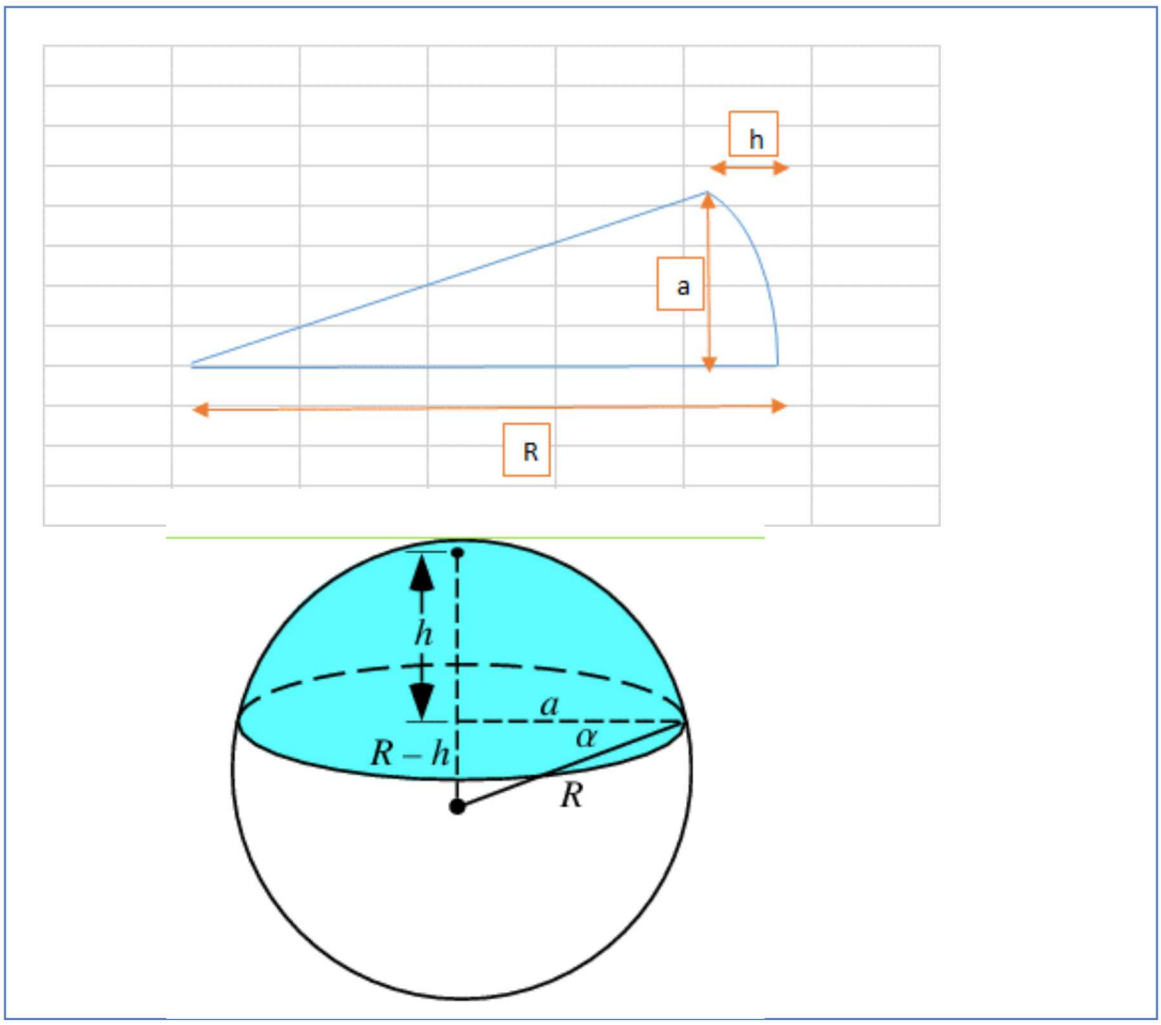

Figure 4. Sketch for volume of end-cap [7]

Combining all of these contributors to the volume, the calculated total volume of the door ranges from 0.3110 m^3 to 0.3172 m^3.

2.2. The Far End Hemisphere

The far end hemisphere was also measured using the Faro laser tracker. The coordinate frame was set to the door flange of the chamber. For this measurement, no cylindrical section was considered since the cylinder is calculated separately [6]. This measurement is only a hemisphere with a truncated cap removed.

The reported hemisphere diameter is 1007.274 mm, and with a minimum and maximum deviation of 11.385 mm; therefore, the minimum diameter is 1001.5815 mm; max diameter is 1012.9665 mm.

The same truncation geometry is used to calculate the volume of the end hemisphere. The calculated end hemisphere volumes range from 0.262 m^3 to 0.271 m^3.

2.3. The Cylinder Body

The volume of the main body of the chamber was also determined. It should be noted that the main cylinder body included 8 triangular ledges used to support the fiber grate. The cylinder body was measured using the Faro laser tracker. Scans were made of 4 of the 8 supporting triangular ledges. The volume of the cylinder body is the volume of the cylinder itself, minus the triangular ledges and minus any additional equipment placed in the chamber, such as equipment grate support, microphones, cables, etc.

Each of the triangular ledge supports are modeled as a prismatic triangle with a specific length, width, and height (volume = L×W×H/2); in addition, each ledge support contains 3 weld beads (V1, V2, H). Each bead was also modeled as a half-cylinder of diameter "Width" and length "Length". Based on the Type B evaluation of the scanner, ± 0.013 mm was used as the uncertainty for the scanner to add or subtract from the prismatic triangle, but the weld bead volumes were not added or subtracted.

The cylinder body's volume ranges from 0.832 m^3 to 0.844 m^3.

The final volume of the acoustic chamber was determined to be 1.419 ± 0.014 m^3. Note that this assumes a rectangular distribution for the uncertainty. Converting this uncertainty to a normal distribution yields the value, 1.419 ± 0.016 m^3 with a confidence level of 95.54% and a coverage factor of k=2. The contributions to this volume calculation are summarized below in Table 1. Also shown below in Table 1 is the calculated interior surface area for the acoustic chamber. In addition, this includes the ledge supports for the grating, and an assumption of a flat cap used to seal the door speakers. This does not include the grating, the access ports for instrumentation or the door speakers. This is a relative uncertainty of approximately 1%. The dominant source of uncertainty is the geometry of the cylindrical body itself; its out-of-roundness (non-spherical) is the largest contributor. To obtain a reduced volume uncertainty, a higher density scan/track of the cylinder itself should be performed.

Table 1: Calculated Acoustic Chamber Volume, all uncertainties below are reported with a confidence level of 95.54% and a coverage factor of k=2

	Volume (m^3)	Interior Surface Area (m^2)
Door Hemisphere:	0.314 ± 0.004	3.328 ± 0.026
Far End Hemisphere:	0.266 ± 0.005	1.509 ± 0.021
Cylinder Body:	0.838 ± 0.007	4.908 ± 0.028
Acoustic Chamber Volume:	**1.419 ± 0.016**	**9.744± 0.075**

3. DETERMINING THE VOLUME OF PERMANENT TEST FIXTURES

A fiber-reinforced grate was another component of the system in which a volume calculation was required. In order to do so, the density of the fiber was needed. Asset # SNL-50047 was used to perform the measurements of the mass of the fiber-reinforced grate used inside of the acoustic chamber.

For the Mettler-Toledo Model PS60 Balance, the stated accuracy is ± (0.1% of reading + 0.05 lb). This is a tolerance and can be treated as a rectangular distribution. The exact conversion from

pounds (avoirdupois) to kilogram is: 4.535 923 7 x 10^{-1} (from NIST SP 811), in kilograms. Therefore, the accuracy can be restated as ± (0.1% of reading + 0.0227 kg), and the mass of the fiber grate can be stated as 11.48 kg ± 0.0342 kg, again, assuming a rectangular distribution.

The density of a sample of the fiber-reinforced material of the grate was measured by Curt Mowry and Adam Pimentel of organization 01852 in their report GMO-2017-9734. Based on the methods used, we estimate that the entire grate's density is approximately 1590 kg/m^3 ± 31.8 kg/m^3 with a level of confidence of approximately 95.45% and a coverage factor of k=2.

The methods used in estimating the density of the material are not correlated (or very poorly correlated—since all mass calibrations trace to the same master weights) with the method used in estimating the mass of the grate, so the assumption of uncorrelated uncertainties is valid.

The measurement equation for the volume *V* is:

$$V = M/\rho$$

where *M* is the mass and ρ is the density. Applying the Kline-McClintock equation, GUM method for uncorrelated uncertainties [5], the uncertainty can be calculated as follows:

$$u_V = \sqrt{\left(\left(\frac{\partial V}{\partial M}\right)u_M\right)^2 + \left(\left(\frac{\partial V}{\partial \rho}\right)u_\rho\right)^2}$$

Or,

$$u_V = \sqrt{\left(\left(\frac{1}{\rho}\right)u_M\right)^2 + \left(\left(\frac{-M}{\rho^2}\right)u_\rho\right)^2}$$

Using the above equations, the volume of the fiber reinforced grate is 0.00722 m^3, with an uncertainty of 0.000147 m^3. This value is determined using a confidence level of 95.45% and a coverage factor of k=2. This uncertainty is dominated by the density of the unknown of the fiber grate which is approximately 2% relative (expanded) uncertainty.

The relative uncertainty associated with the density of the grate (coverage factor of k=1) is 1%, while the relative uncertainty associated with the mass measurement is 0.17%. There is little to no benefit of looking at the influence of air buoyancy for this measurement (the buoyancy force due to the volume of the grate is about 0.007 kg, or 0.06% of the measured mass). To reduce the uncertainty of the volume of the grate, we have three recommendations: certifying the volume and mass of the steel sphere check standard used for the measurements or use a PSL-certified silicon nitride (SiN) sphere with known volume and mass and/or providing several more samples; each sample should approximately be (1.2×1.2×0.5 cm) to obtain better statistics of the fiber-reinforced grate material.

4. MEASUREMENT OF SPEAKER DISPLACEMENT

The sound source for this acoustic chamber is a speaker (driver) that is controlled using a signal generator to generate sounds at various frequencies and amplitudes. When using a pistonphone, this significantly impacts the internal volume of chambers, so they have a large uncertainty contribution to the overall measurement. In this case, the speaker displacement was measured using the Faro Laser tracker. The change in the internal volume of the acoustic chamber due to the displacement of the driver was found to be insignificant in comparison to the uncertainty of the volume measurement.

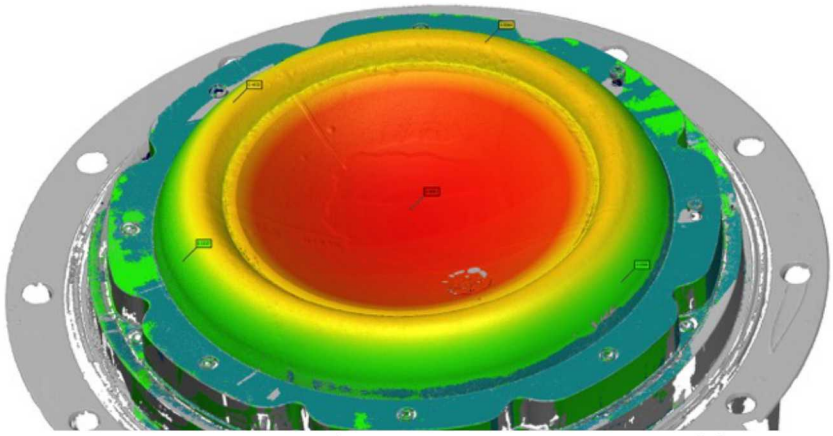

Figure 5: 3D Image of Measurement Result of Speaker

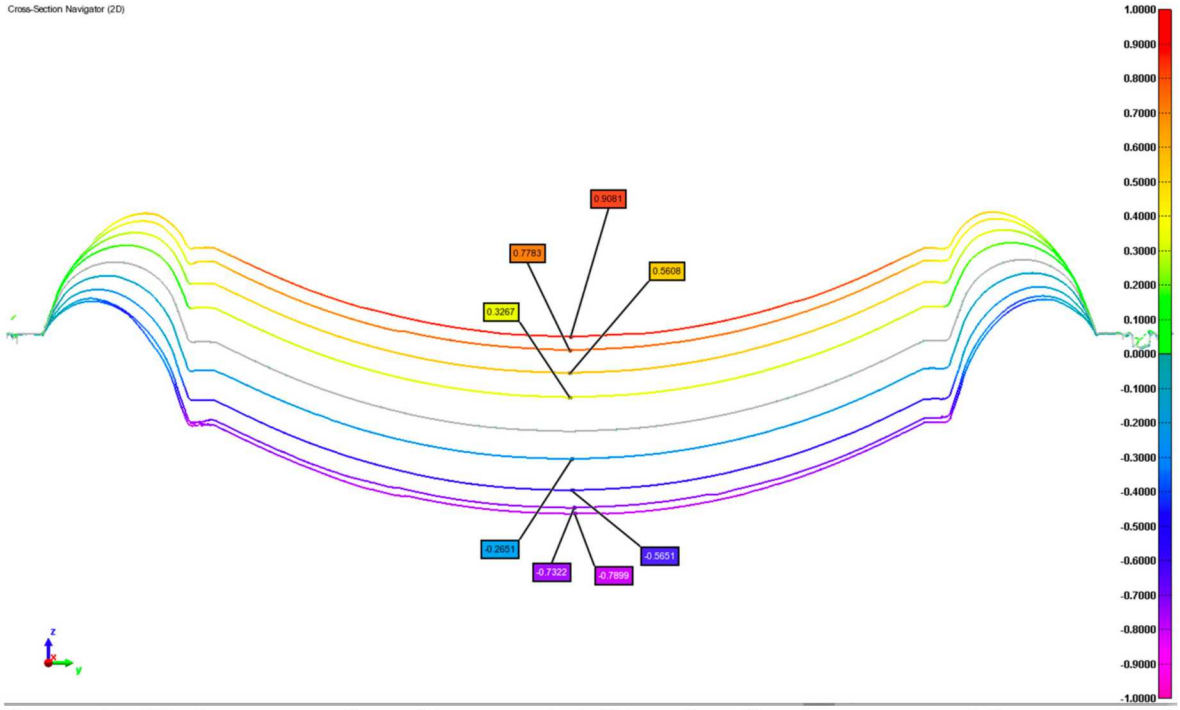

Figure 6: 2D Cross sectional image detailing the displacement of the speaker's diameter (inches) from 0% to 100% of output in both extension and retraction modes.

The change in position caused by operating the speaker from 0% to 100% of the speaker displacement was measured and is shown below in Table 2. The uncertainties (level of confidence of 95.45% with a coverage factor of k=2) reported in Table 2 are based upon the uncertainty of the dimensional measurements. The minimum and maximum flat position reflects the irregularity in the position of the flat ring inside the foam ring during extension and retraction.

Table 2: Change in Flat Position of the Speaker

	Flat Position (mm)				
Speaker Extension	Minimum	Maximum	Median	Mean	Uncertainty (± mm)
100%	22.044	23.670	22.781	22.854	0.025
75%	19.047	20.190	19.517	19.564	0.025
50%	13.789	14.780	14.272	14.272	0.025
25%	7.795	8.887	8.239	8.303	0.025
	Flat Position (mm)				
Speaker Retraction	Minimum	Maximum	Median	Mean	Uncertainty (± mm)
100%	-20.780	-19.637	-20.463	-20.320	0.025
75%	-19.612	-18.367	-18.939	-19.034	0.025
50%	-14.735	-13.694	-14.202	-14.208	0.025
25%	-7.344	-6.150	-6.899	-6.798	0.025

The effective piston area of the speaker is shown below in Table 3. The effective piston area was calculated based off the diameter of the cone and radius of the foam ring at the various speaker positions. The uncertainties (level of confidence of 95.45% with a coverage factor of k=2) reported in Table 3 are based upon the uncertainty of the dimensional measurements.

Table 3: Effective Piston Area of the Speaker

Speaker Extension	Effective Piston Area (m^2)	Uncertainty (± m^2)
100%	0.038611	0.000010
75%	0.038508	0.000010
50%	0.038592	0.000010
25%	0.038501	0.000010
Speaker Retraction	Effective Piston Area (m^2)	Uncertainty (± m^2)
100%	0.038485	0.000010
75%	0.038486	0.000010
50%	0.038569	0.000010
25%	0.038470	0.000010

5. ACOUSTIC CHAMBER ENVIRONMENTAL CHARACTERIZATION

5.1. Internal Temperature Characterization

Changes in temperature cause variations in pressure inside the chamber which can affect the results when calibrating infrasonic sensors. Thus, care must be taken to reduce temperature gradients across the chamber as well as maintain a constant temperature over time. Another important practice is allowing the sensors enough time to reach thermal equilibrium after they have been placed in the chamber. With these considerations, the temperature and pressure stability of this acoustic chamber was evaluated. The results of the temperature measurements were evaluated and will be discussed here. Pressure measurements will also be discussed.

Nine two-wire 30,000 Ω thermistors were mounted inside the chamber at various points so that the temperature was closely monitored. These 30,000 Ω thermistors were calibrated at the FACT site using a thermal dry well and referenced against a two-wire 10,000 Ω thermistor calibrated by the PSL Temperature Laboratory. The data acquisition system for these measurements was an Agilent 34972A. The 10,000 Ω thermistor (PSL asset # 6671836 and/or 6671796) was calibrated by measuring the resistance at two fixed temperature points and one comparison point with a Standard Platinum Resistance Thermometer (SPRT). The resistance measurements were made using a Fluke 8508A Reference Multimeter. The temperature points were certified using the triple point of water of approximately 0.01 °C, the comparison point of 15 °C and the Gallium Melting Point of approximately 29.7646 °C. The 10,000 Ω thermistor has a time of test uncertainty of 0.083 °C and an interval uncertainty of 0.25 °C with a confidence level of 95.54% and a coverage factor of k=2.

The contributors evaluated for the combined uncertainty for the temperature measurements includes the Type B contributor from the 10,000 Ω thermistor of 0.125 °C and the thermistors manufacturers specification for repeatability (accuracy) of these thermistors of 0.2 °C. Since this accuracy does not state the distribution, it is safe to assume that it is a rectangular distribution [5]. The repeatability of the measurements at time of test was quite low since we had a long dwell time based upon the repeatability of the measurements during the calibration. Applying the Kline-McClintock Equation [5]:

$$u_V = \sqrt{\left(\left(\frac{0.2}{\sqrt{3}}\right)\right)^2 + \left(\left(\frac{0.25}{2}\right)\right)^2} * 2 = 0.34\ °\text{C}$$

The uncertainty for the temperature measurements made using each of the nine 30,000 Ω thermistors is 0.34 °C with a level of confidence of 95.54% and coverage factor of k=2. The positioning and labeling of each of the nine 30,000 Ω thermistors are shown below in Figure 7. These channel numbers will be referenced for the graphs and data discussed in this report.

Channel	Location
101	Top Front (by door)
102	Top Rear
103	Right Front (aligned with door flange upper right bolt)
104	Right Rear (aligned with side center)
105	Left Front (aligned with side center)
106	Left Rear (aligned with upper left bolt)
107	Rack Front (suspended from grate, front center)
108	Rack Rear (suspended from grate, near center)
109	Bottom Center (centered on bottom, front to rear)

Figure 7: Position of mounted 30,000 Ohm Thermistors

As was previously mentioned, temperature is an important factor in acoustic measurements. Figure 8 shows the first attempt at measuring the temperature of the acoustic chamber along with the ambient room temperature. These measurements were performed for about four days with only the thermistors, cabling, and the test rack inside of the chamber. This was performed to obtain a baseline for the temperature and pressure of the chamber. The temperature of the chamber follows closely with the ambient temperature of the room. This was quite problematic since there were significant fluctuations from day to night and the acoustic chamber never had a chance to truly stabilize to one temperature.

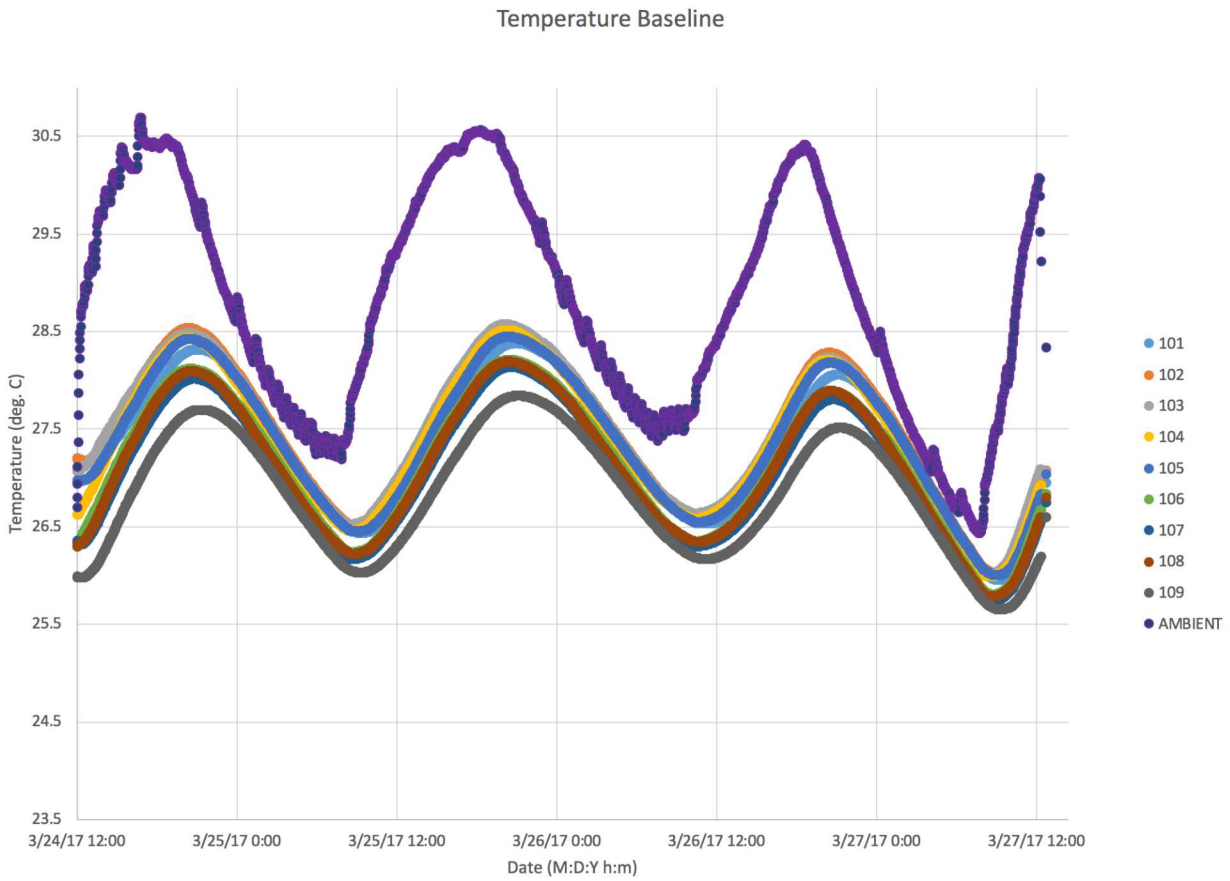

Figure 8: Baseline Temperature Data

Building SB-1, where the acoustic chamber is located, originally had no functioning environmental controls. After reviewing these results, improvements in the environmental controls were introduced to both the building as well as the chamber. The building had the heating, ventilation and air conditioning (HVAC) unit repaired to ensure a controlled temperature for the room. The acoustic chamber had a heating pad externally installed on both the top and bottom of the chamber, each with an external control. Figure 9 shows the baseline temperature after making these changes with the HVAC offset to 20 °C. The amount of time that the door to SB-1 was opened was also minimized in order to better control the temperature of the building. For the baseline, the heating pads were not turned on. The data shows that the temperature still follows the ambient conditions of the room, however the temperature gradient of the chamber is minimal with all thermistors within 1 °C of each other. Figure 10 shows the internal temperature of the acoustic chamber with the heating pads turned on. The top heating pad was set to 23.5 °C and the bottom heating pad was set to 22.5 °C. With the heaters on, it is still possible to see the internal temperature of the chamber fluctuating with the ambient temperature, however, the overall temperature of the chamber remained relatively steady a 22.5 °C. Also, the overall gradient of the internal temperature of the chamber has been increased with this configuration.

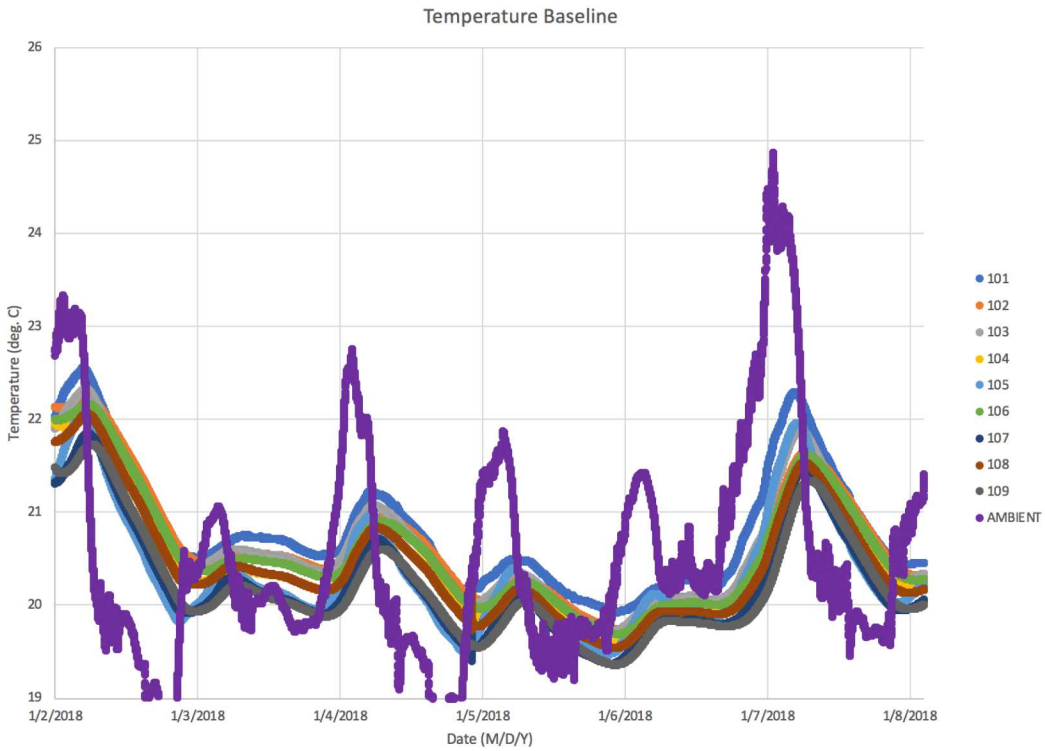

Figure 9: Baseline Temperature, Post Changes

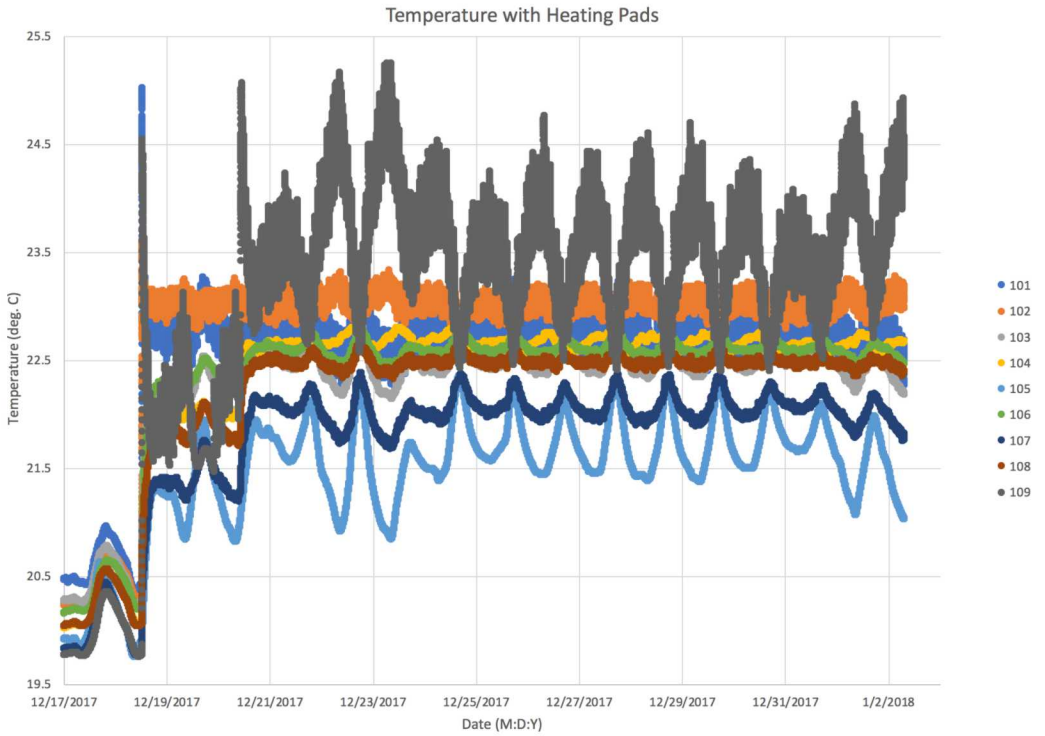

Figure 10: Internal chamber temperature with heating pads turned on

In addition to measuring the temperature at ambient conditions, the temperature was also measured when all electronic equipment within the chamber was powered on. The following equipment was turned on during testing: MB2000 Infrasound Sensor, Hyperion 5000 Infrasound Sensor,

Chaparral 50A Infrasound Sensor, Vaisala PTU300 and a B&K power supply with two microphones attached. The chamber temperature was monitored for the duration of one week for these tests. During these measurements, there was no significant deviation from the data shown in Figure 10. The variation due to the ambient temperature of the room heavily outweighed the contribution of the heat load to the point where deviations between the two are not easily noticed.

To simplify the future use of the thermistors, circuits that can convert the coefficients for the 30,000 Ω thermistors to a corresponding output voltage in real time were evaluated. The Acromag TT334 Transmitter was determined to be a suitable commercial off the shelf piece of equipment that would accomplish this task. The TT334 transmitters converts the resistive sensor input to a proportional control signal and has an accuracy of ± 0.05 °C.

The internal temperature of the acoustic chamber was evaluated and controlled to a tolerance of 23 ± 3 °C. To improve the temperature control, reduction of the temperature gradient in the chamber should be evaluated. When performing calibrations using this acoustic chamber, it is important to monitor and track the temperature to ensure that it remains within the stated tolerance at the setpoint. It is important to standardize test conditions so that results across different laboratories can be easily compared.

5.2. Internal Pressure Characterization

The internal pressure of the chamber was evaluated using a Setra Model 278 Pressure Transducer, PSL asset # 6676085. The external temperature of the chamber was measured using a Vaisala PTU303 barometric pressure sensor, PSL asset # 6676085. The Vaisala has an interval uncertainty of 15 Pascals with a confidence level of 95.45% and a coverage factor of k=2. The Setra Model 278 Pressure Transducer has an interval uncertainty of 0.6% with a rectangular distribution.

The initial pressure measurements are shown below in Figure 11. The internal chamber pressure closely followed the ambient pressure. The post environmental control changes described above are shown in Figure 12. There is a decrease in the rate of change for the internal pressure in response to the ambient pressure. It is important to note that the change in ambient pressure is minimized to reduce the impact of this on the calibration results.

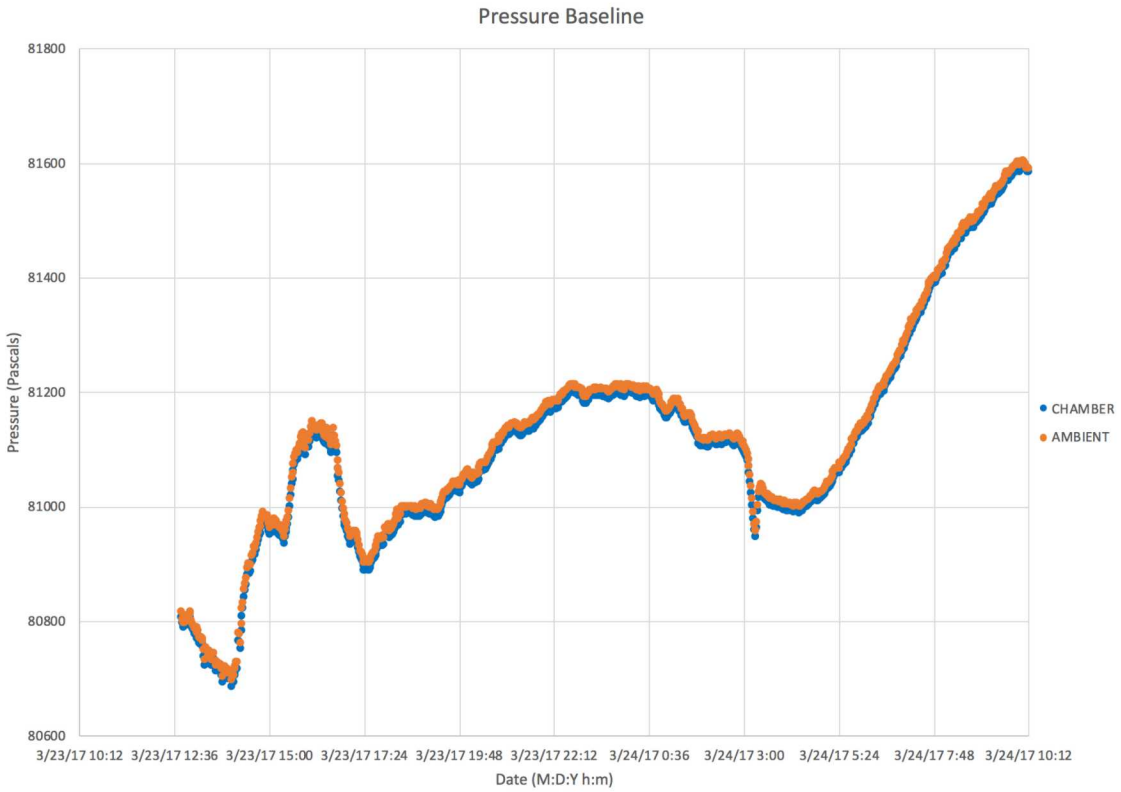

Figure 11: Initial Pressure Baseline

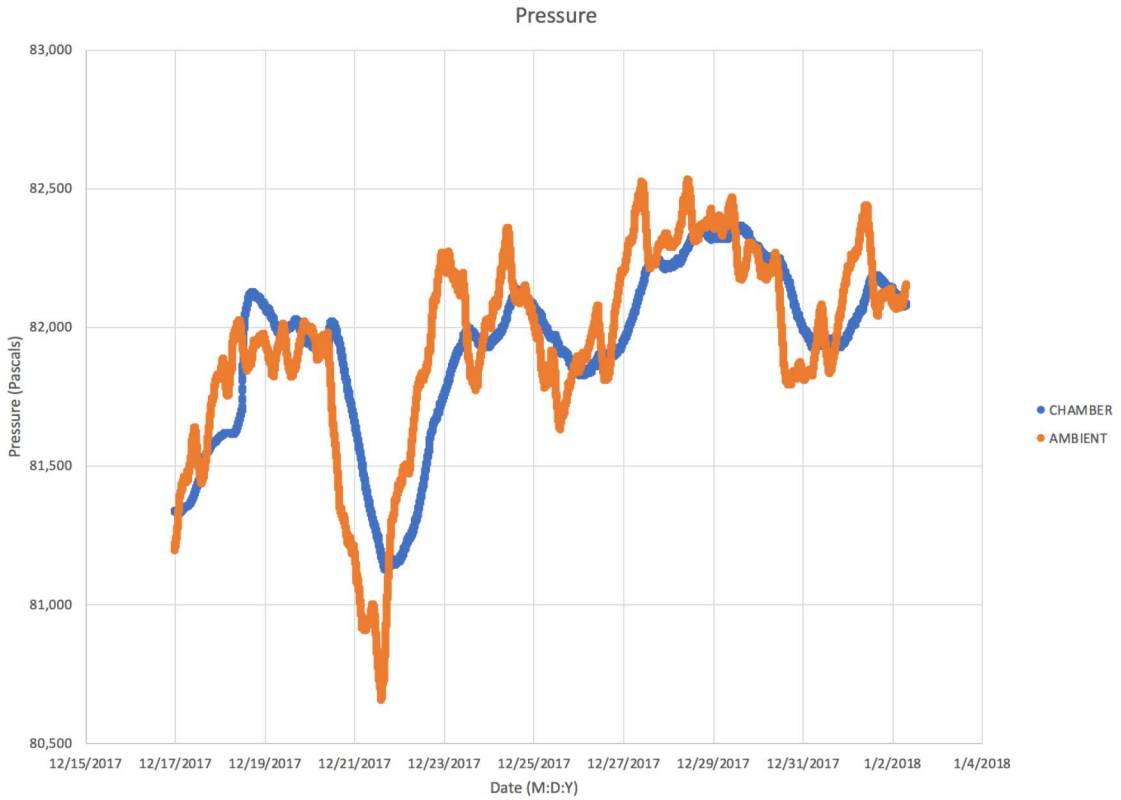

Figure 12: Post-changes Pressure Baseline

5.3. Acoustic Chamber Leak Rate

The chamber was pressurized to approximately 1 atmosphere, 103 kPa relative to ambient conditions of 81 kPa. and the bleed down time was measured. The pressure response of the chamber during this leak test is shown below in Figure 13. The calculated leak rate was approximately 1339 sccm for the first nine hours and 920 sccm for the next 24 hours. This discrepancy was troubling, and after further testing, it was determined that the chamber was leaking through the cables going through the bulk head adapter. The leak issues were resolved by improving these connections through the bulkhead. Additional pressurization data was not taken and analyzed but appeared to have drastically improved. It is recommended to perform this test again and calculate a new leak rate for the acoustic chamber. It is also important to perform this test again when the speaker is connected and functioning to ensure that there are no additional leaks in the final system configuration.

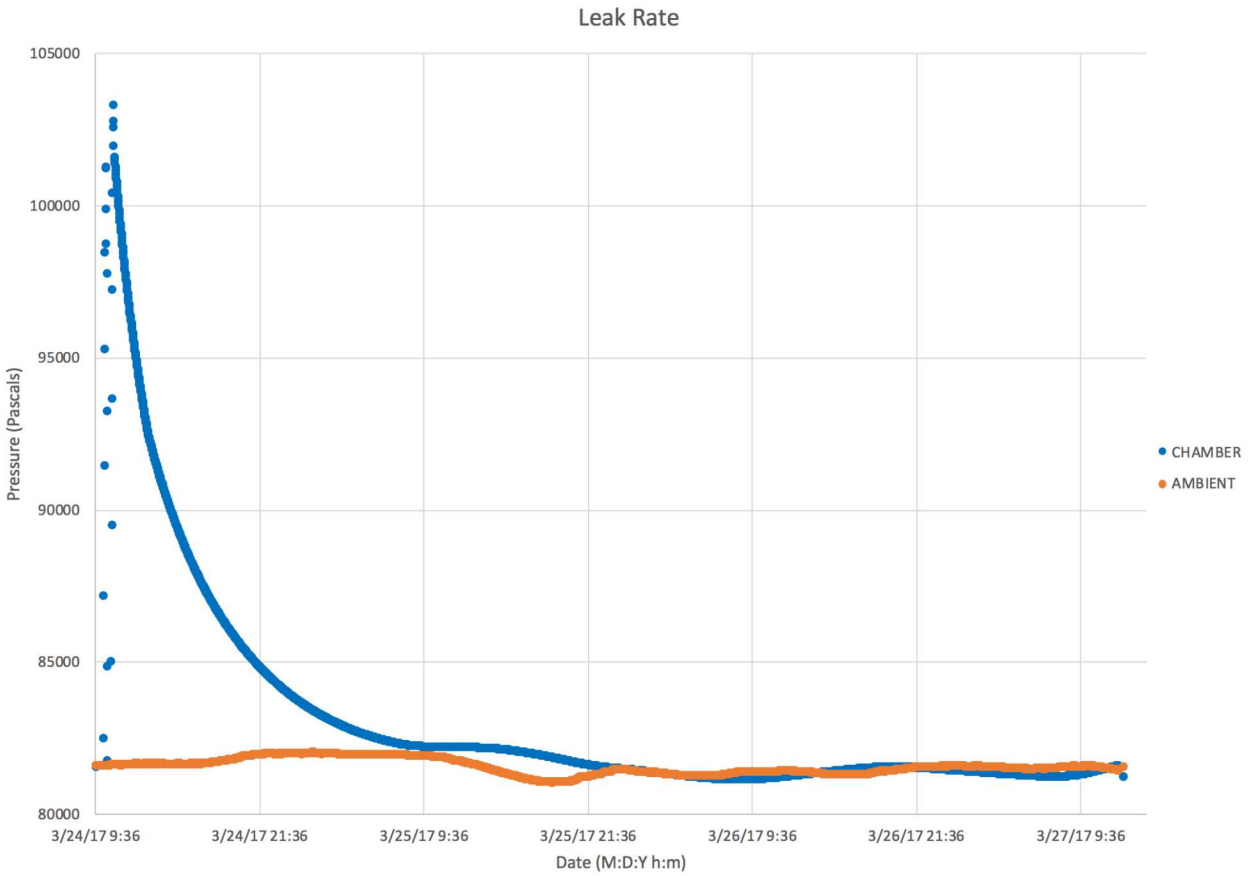

Figure 13: Acoustic Chamber Original Leak Rate

6. RESONANT FREQUENCY OF THE ACOUSTIC CHAMBER

The resonant frequency of the chamber must be determined to ensure it is well outside the range of the measurements being performed. Chamber resonant frequency measurements were

performed using a working standard microphone system with IEC type WS2F. This microphone was optimized for low frequency operation. GRAS Type 40AN; serial no 42875. The microphone was calibrated by the National Physical Laboratory (NPL) using the NPL laser pistonphone following the model given in IEC 61094-2. The microphone was calibrated down to a frequency of 1 Hz and had a reported sensitivity level of approximately -26 ± 1 dB re 1 V per Pa. The resonant frequency of the acoustic chamber without extra infrasonic sensors powered on in the system was approximately 95.0 Hz, as shown in Figure 14. The resonant frequency was approximately 96.5 Hz when the extra sensors were not in the acoustic chamber, as shown in Figure 15.

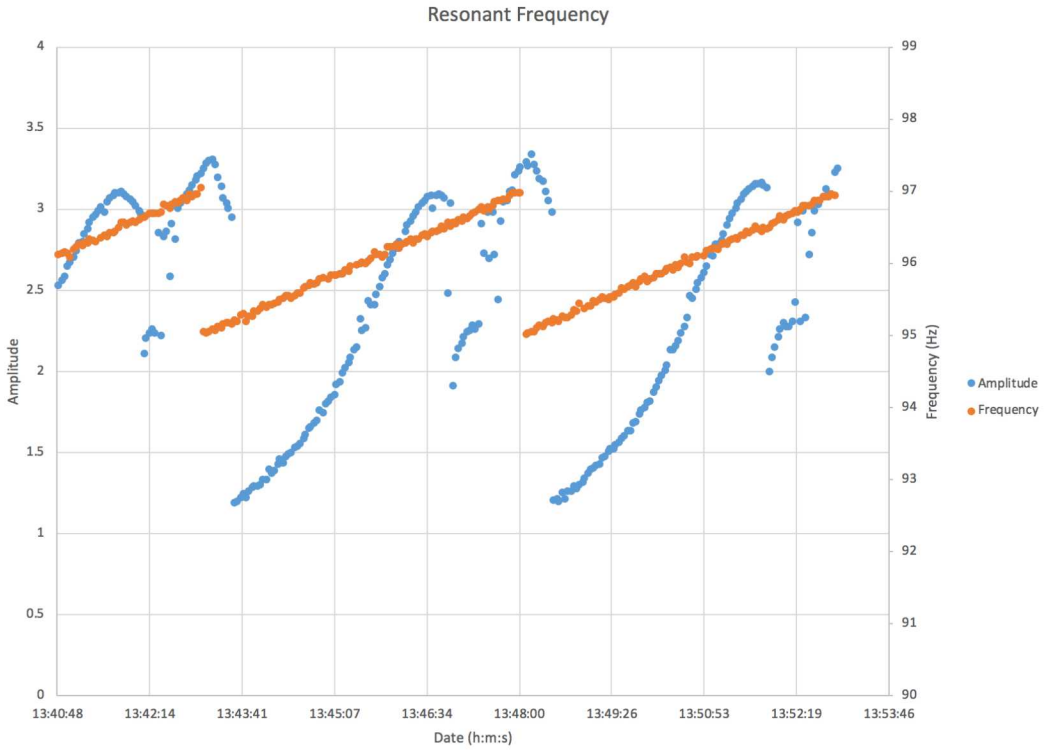

Figure 14: Resonant Frequency without any infrasound sensors adding for heat affects

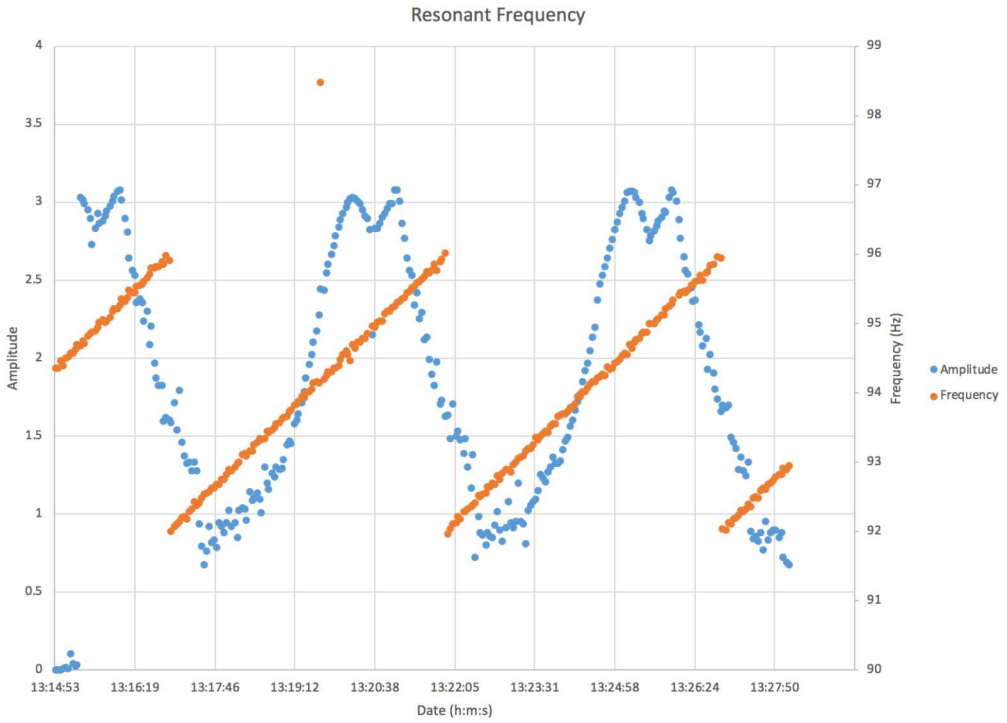

Figure 15: Resonant Frequency with added infrasound sensors

7. CONCLUSION

The major uncertainty contributors of the acoustic chamber located at the FACT site were evaluated. The internal volume of the chamber was determined to be 1.419 ± 0.014 m^3. The internal temperature of the chamber was determined to be stable within 23 ± 3 °C when the heating pads are in use. The internal pressure of the chamber was evaluated, and a leak was detected. It is recommended that additional leak tests are performed to evaluate a new leak rate for the chamber. The resonant frequency of the chamber was evaluated, and it is much greater than the frequency band of interest for infrasound calibrations. As described above, it is important that standardized conditions are used going forward and that these conditions are reported along with the reportable data. Since this work is still in the developmental phase, no procedures were reviewed or finalized. Once the measurement method is determined along with its associated measurement equation, the uncertainties provided in this report should be carried forward.

REFERENCES

[1] C. Talmadge, "NCPA Laboratory Calibration Description," University of Mississippi, 2015.

[2] US Infrasound Calibration Team, "Guidelines for Infrasound Sensor Characterization and Calibration".

[3] IEC 61094-2, "Electroacoustics - Measurement microphones," International Electrotechnical Commission, Switzerland, 2009.

[4] IEC 61094-5, "Electroacoustics - Measurement microphones - Part 5: Methods for pressure calibration of working standard microphones by comparison," International Electrotechnical Commission, 2016.

[5] JCGM 100:2008, "Evaluation of measurement data - Guide to the expression of uncertainty in measurement," JCGM, 2008.

[6] U. o. M. Professional Drawing from National Center for Physical Acoustics, *Calibration Tank Assm 2014_Casters-Grates-Tank Flange,* 2015.

[7] E. Weisstein, "MathWorld - A Wolfram Web Resource," [Online]. Available: http://mathworld.wolfram.com/SphericalCap.html. [Accessed 22 May 2018].

This page left blank

DISTRIBUTION

Email—Internal

Name	Org.	Sandia Email Address
John Merchant	06752	bjmerch@sandia.gov
Randy Rembold	06752	rkrembo@sandia.gov
Hy Tran	09100	hdtran@sandia.gov
Roger Burton	09143	rburto@sandia.gov
Timothy Kypta	09143	tkypta@sandia.gov
Edward O'Brien	09143	edobrie@sandia.gov
Joshua Stanford	09143	jstanfo@sandia.gov
Technical Library	9536	libref@sandia.gov

This page left blank

This page left blank

Sandia National Laboratories

Sandia National Laboratories is a multimission laboratory managed and operated by National Technology & Engineering Solutions of Sandia LLC, a wholly owned subsidiary of Honeywell International Inc. for the U.S. Department of Energy's National Nuclear Security Administration under contract DE-NA0003525.